Research Article

Experimental Investigations into Effective Parameters for Improvement of Current Density in Microbial Fuel Cells

Mina Bahraminasab [a], Hamed Moqtaderi [α,*], Atieh Kiaeinejad [a]

[a] Department of Mechanical Engineering, Faculty of Engineering, Alzahra University, Tehran, Iran.

ABSTRACT

Microbial Fuel Cells (MFCs) represent an environmentally-friendly approach to generating electricity, but the need to study variation parameters to find improvement conditions has been an important challenge for decades. In this study, a single-chamber MFC was designed to investigate the key parameters such as the concentration and type of bacteria, chamber temperature, electrode spacing, and substrate rotation speed that affected the performance of MFCs. Therefore, two types of bacteria, Shewanella oneidensis (S.one) and Escherichia coli (E. coli), were compared as microorganisms. Then, the function of MFC was investigated under the following condition: three temperatures (30 °C, 45°C, and 60°C), three bacterial concentrations (0.5% (v/v) (4.5 mg/ml), 1% (v/v) (9mg/ml), and 1.5% (v/v) (13.5mg/ml)), electrode distances (2 cm, 3 cm, 4cm), and substrate speeds (100 rpm, 150 rpm, 200 rpm). Ultimately, (S.one) bacteria, a chamber temperature of 45 °C, a bacterial concentration of 1% (v/v) (9mg/ml), a cathode-anode spacing of 3 cm, and a rotation speed of 150 rpm proved to be the most efficient parameter settings for the constructed microbial fuel cell. The maximum voltage and highest power density were 486.9 mV and 9.73 mW/m^2, respectively, with a resistance of 7500 ohms. These results are meaningful for determining and improving important parameters in an MFC device.

1. INTRODUCTION

As the energy crisis is one of the most significant problems, much attention has been paid to the development of sustainable energies recently (Mishra et al., 2017). The sustainable energy source is a type of energy that has no threat of being ruined in the future (Cui, 2016), and the method of generating electricity from renewable energies has been discovered some years ago (Keshavarz et al., 2022). Fuel cells are one of the renewable resources that convert chemical into electrical power and according to their main contributions that impact the performance, catalysts, electrolytes, and temperature range are generally categorized (Pandey, 2019). The Microbial Fuel Cell (MFC) is a device that converts chemical into electrical energy environmentally by using microorganisms as catalysts (Cao et al., 2019). This device generates useful products like hydrogen (Walter et al., 2020), but for using hydrogen as a source of energy, the method of hydrogen storage is an important issue (Tabrizi et al., 2019). In MFC technology, the electrodes, membrane, and bacteria acting as a biocatalyst are the main components (Obileke et al., 2021). Bacteria oxidized the organic matter in an anodic chamber to generate electricity

(Salar-García & Ieropoulos, 2020). Transferring electrons to the cathode by an external circuit and protons through the membrane makes a potential difference between the electrodes that contribute to electricity generation (Dessie et al., 2020). Numerous studies have been done over decades to increase anode-specific surface area and electron transfer rates in MFCs (Gajda et al., 2020). In microbial fuel cells, the anode electrode acts as a direct electron acceptor since electrons accumulate on the surface of the anode electrode and travel through the external circuit to the cathode electrode. At the same time, the cations migrate through the electrode from the anode to the cathode via the electrolyte (Mateo et al., 2018).

Attempting to improve the MFC design is an issue that researchers are still working on (Chhazed et al., 2019). Usually, there are two types of MFCs: single-chamber and dual-chamber designs (Oliot et al., 2017). In a single-chamber design, the porous cathodes are formed on one side of the cathode chamber to utilize atmospheric oxygen and allow protons to diffuse through them. In contrast, in a dual chamber design, a membrane separates the electrodes (Jumma & Patil, 2016). The design has played a crucial role in this technology because the function, practical applications, and cost depend on an

appropriate design (Salar-García & Ieropoulos, 2020). Therefore, researchers have recommended various high performances (Mishra et al., 2017). Since the main goal is to achieve higher efficiency (Paez et al., 2019; Nguyen et al., 2020), the focus must be on the factors that affect the power output, such as substrate, temperature, and cell configuration (Mei et al., 2017; Ezziat et al., 2019). In this study, a single-chamber or air-cathode MFC was designed and constructed. Due to the clearer energy supply and the development of sustainable waste management systems, MFCs have received much attention (Obata et al., 2020). Since the single-chamber design does not require a separate cathode chamber, the design is more straightforward and the cost decreases; thus, they are more commonly used in the industry. Even though the improvement of the MFCs performance has increased significantly in various research areas, the published reports on the impact of studying all the important parameters on power generation are still limited, and most of the works in the literature so far have mainly focus on either one physical property or one and two effective parameters. For these reasons, this work aims to evaluate multiple parameters to maximize the power generation for a single chamber MFC and make it simple and cost-effective. In this regard, the effects of bacteria, chamber temperature, bacteria concentration, electrode distances, and substrate rotation speed on the MFC performance were investigated.

In the following, Section 2 describes the properties of the chamber and the method used to construct its particles. In addition, Subsections 2.1-2.7 describe the method used to prepare the main components, electrodes, membrane, and substrate. Subsections 2.8-2.9 explain types of bacteria, how to provide them, test methods, and data recording. Section 3 explains the results of the tests for each parameter separately. Finally, Section 4 presents the conclusions and future research.

2. MATERIALS AND METHODS

In the present work, a single-chamber microbial fuel was designed due to its advantages compared to a double-chamber one, such as cost efficiency, higher power generation, and ease of aeration of the cathode chamber (Tan et al., 2020). All its particles were drawn from Solid Works software, and laser cutting and CNC machines were employed to precisely cut the particles. In addition, chloroform was used to seal the chamber.

The chamber is a rectangular prism with dimensions 160 mm × 60 mm × 60 mm. Figure 1(A) shows some grooves on the inner side of the chamber wall to let the anode be at 23 mm, 32 mm, and 42 mm distances from the cathode. Figure 1(B) depicts an array of 5-mm holes to create an air contact on the cathode side wall of the chamber. Figure 1(C) shows a T-shape plexiglass to accommodate the anode-bearing rod at different distances from the cathode. Figure1(D) represents a cover on the top of the chamber with a 5mm hole to provide anaerobic

conditions with easy access to the interior parts of the cell and let a wire connect the anode electrically to the external devices.
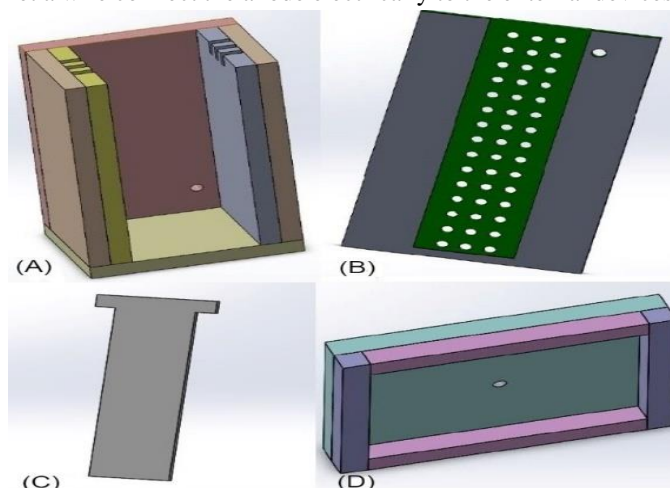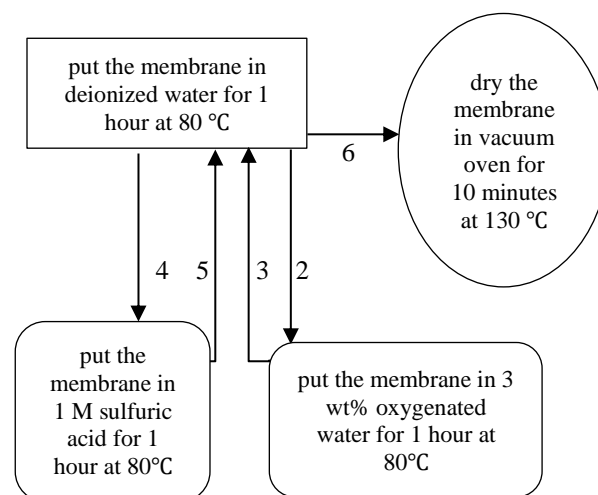

Figure 1. (A) Single Chamber, (B) Pores of 5 mm, (C) T-shape Plexiglass, and (D) A door on the top of the chamber

2.1. Membrane

An ion exchange membrane separates two electrodes and prevents oxygen from passing through the anode electrode (Koók et al., 2021). In this study, the membrane is Nafion 115 with dimensions of $150 \times 32 \times 0.127$ mm. Formation of a direct connection between the cathode and the membrane enhances their separation (Koók et al., 2021). Before using the Nafion, a process is necessary to remove impurities and increase the porosity of the membrane. First, the membrane was placed in deionized water and, then, in 3 wt% oxygenated water. After that, the first step is repeated. Then, the membrane is placed in a 1 M sulfuric acid solution. Finally, to prepare the membrane, the first step is repeated. It is necessary to mention that the temperature in each step is 80 °C, the duration takes 1 hour, and the Nafion is floating in the solution during all the steps (Note: when it comes to the use of the Nafion, it is dried in a vacuum oven at 130 °C for 10 minutes). Flowchart 1 shows the steps to prepare the membrane.

Flowchart 1. the steps to prepare the membrane

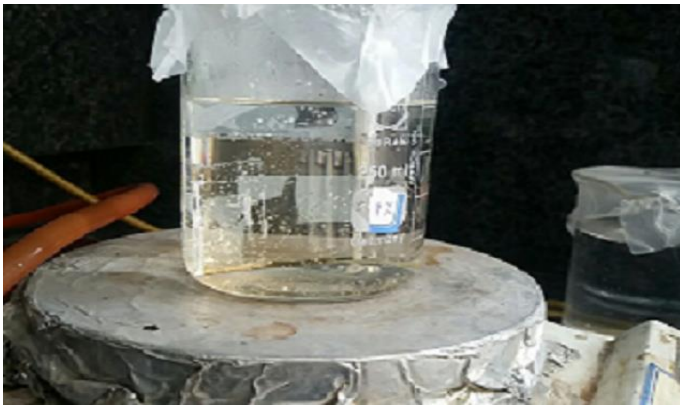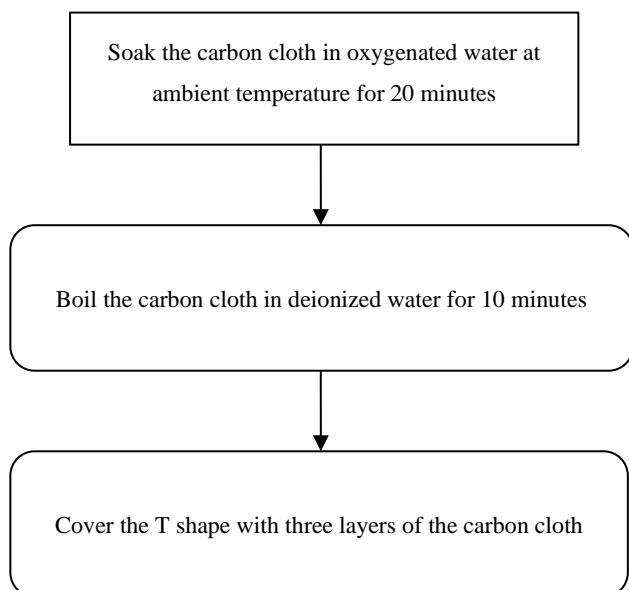Figure 2 represents the procedure of the membrane preparation.

Figure 2. the procedure of preparing the membrane

2.2. Anode Electrode

Anode plays a key role in making bacterial biofilm; hence, a proper anode is rich in electrical conductivity and has a high specific surface area (Gajda et al., 2020). There are various carbon-based materials for the anode, such as carbon cloth, felt, and brush (Gajda et al., 2020). In this study, both electrodes are characterized by carbon cloth and some steps are necessary to prepare the electrodes before use. Therefore, the anode electrode was soaked in oxygenated water at ambient temperature for 20 minutes and, then, it was boiled in deionized water for 10 minutes to remove contaminants accumulated inside its pore. Three layers of carbon cloth cover the T-shape anode to achieve an appropriate carbon cloth thickness. Flowchart 2 shows the steps of preparing the Anode.

Flowchart 2. Steps of preparing the anode

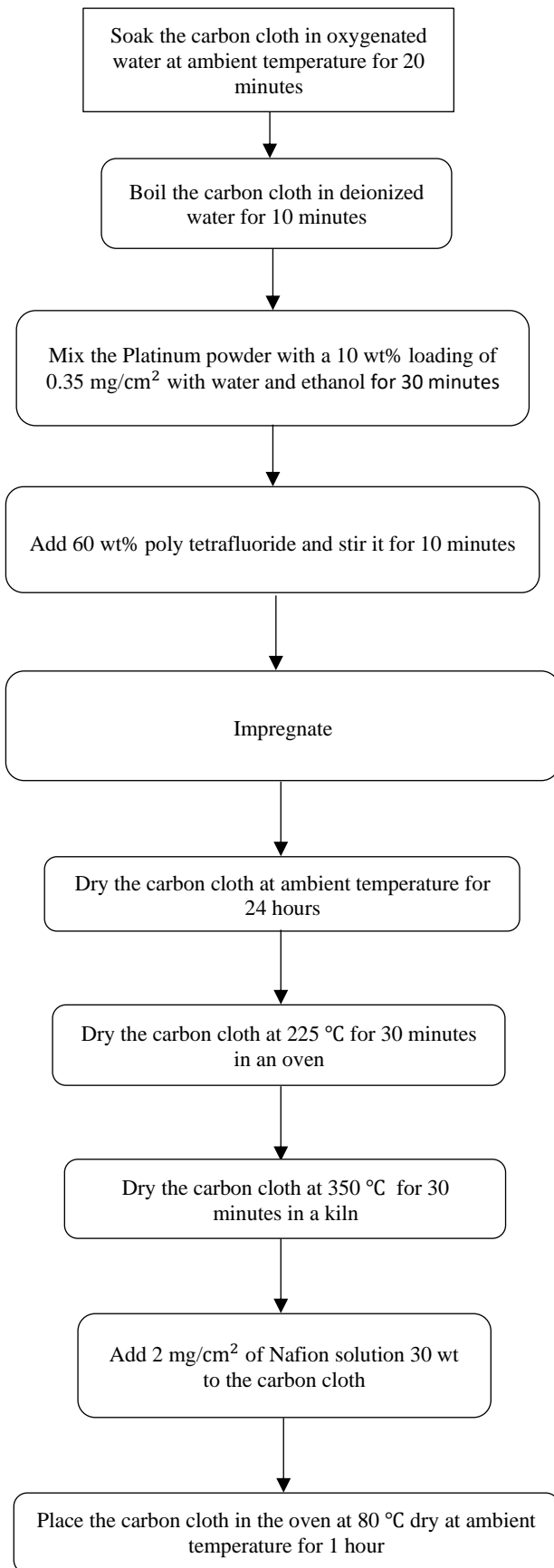Figure 3 presents the procedure of preparing the anode.

Figure 3. The procedure of preparing the anode

2.3. Cathode Electrode

The first step in making the cathode electrode is the same as that in the anode electrode. Although oxygen is the best-known and most suitable electron acceptor, carbon-air cathodes suffer low efficiency due to the slow kinetics of oxygen reduction in carbon cathodes. Therefore, additional stages are required for the cathode to increase the efficiency in a single-chamber MFC. A common technique, Pt/C catalyst, was used to solve the problem, accelerate the oxygen recovery, and reduce the over potential at the cathode (Li et al., 2021). Thus, platinum powder with a 10 wt% loading of 0.35 mg/, water, and ethanol was mixed for 30 minutes. Next, 60 wt% of the ordinary polymer binder in the fabrication of metal-carbon composite electrodes, Polytetrafluoroethylene (PTFE) (Simeon et al., 2022), was added to make a 30 wt% solution and stirred for 10 minutes. After that, the surface of the air cathode with dimensions 150 mm $\times$ 32 mm $\times$ 2.53 mm, as shown in Figure 4, was impregnated with the prepared mixture and a brush.

Figure 4. Air cathode preparation

Soak the carbon cloth in oxygenated water at ambient temperature for 20 minutes

↓

Boil the carbon cloth in deionized water for 10 minutes

↓

Mix the Platinum powder with a 10 wt% loading of 0.35 mg/cm² with water and ethanol for 30 minutes

↓

Add 60 wt% poly tetrafluoride and stir it for 10 minutes

↓

Impregnate

↓

Dry the carbon cloth at ambient temperature for 24 hours

↓

Dry the carbon cloth at 225 ℃ for 30 minutes in an oven

↓

Dry the carbon cloth at 350 ℃ for 30 minutes in a kiln

↓

Add 2 mg/cm² of Nafion solution 30 wt to the carbon cloth

↓

Place the carbon cloth in the oven at 80 ℃ dry at ambient temperature for 1 hour

Flowchart 3. The steps required to prepare the cathode electrode

In the following, the carbon cloth was dried in three stages: at ambient temperature for 24 hours, at 225 ℃ for 30 minutes in an oven, and then, in a kiln at 350 ℃ for 30 minutes. Finally, 2

mg/cm² Nafion solution (30 wt%) was added to the carbon cloth. The carbon cloth was placed in the oven at 80 ℃ and dried at ambient temperature for 1 hour. Flowchart 3 shows the steps to prepare the cathode electrode.

2.4. Membrane and Electrode Assembly

After preparing the membrane and electrodes, several layers of carbon cloth were pressed onto the membrane for 15 minutes at 145℃ temperature and 193 atm pressure (Kiaeenejad et al., 2020). In the end, two copper wires were attached to the surface of each electrode to make a circuit. Figure 5 shows an exploded view of the cathode electrode in Solid Works software.
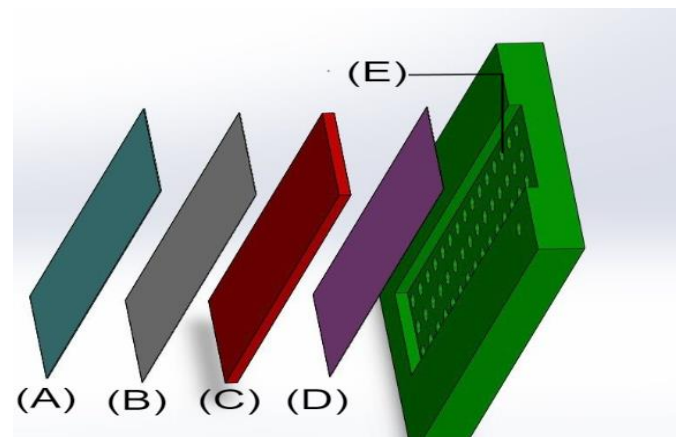

Figure 5. Exploded drawing view of the cathode electrode (A) membrane, (B) nafion+PTFE+Pt powder, (C) cathode, (D) Pt Powder

2.5. Chemicals

For making a 0.4 M NaOH solution, 5 g of crushed NaOH was added to 250 ml of deionized water and stirred until being completely dissolved.

2.6. Reducing Agent

The reducing agent is mandatory in eliminating extra oxygen in the chamber (Cui, 2016). First, 25 mL of 0.4 M NaOH solution was poured into a small storage. Second, while the storage was in a fume hood to aerate the solution with N_2 gas, 1.35 g of cysteine HCl, 20 mL of 3 (w/v%) Na_2S, and 5 mL of DI water were added to the storage. It should be noted at this point that 50 mL of the reducing agent was added to 1 mL of the substrate, which will be described in the next step.

2.7. Substrate

One of the most impressive MFC component required for electricity generation is substrate, which is of different types, ranging from pure compounds to complex substrates, such as wastewater (Salar-Garcia et al., 2021). In this study, some components are combined according to the following steps to produce the substrate. First, 1 L of DI water was poured into

the reservoir containing 5 g of sodium acetate and then, the solution was located on a magnetic stirrer at 400 rpm. Next, the compounds mentioned in Table 1 were added to the reservoir, respectively.

Table 1. Components of the substrate

Component	Formula	Amount
Dipotassium phosphate	K2HPO4	0.9 g
Ammonium chloride	NH4Cl	0.73 g
Sodium chloride	NaCl	0.9 g
Magnesium sulfate	MgSO4	0.09 g

When all particles dissolved, the N_2 gas tube was inserted into the storage for 10 minutes and then, 50 ml of the reducing agent was slowly added to the reservoir. At this point, HCl and NaOH were used to adjust the pH of the solution to 6.8 (Cui, 2016).

2.8. Bacteria

Bacteria adhere to the surface of an anode and form a biofilm that protects a microorganism from environmental threats (Greenman et al., 2022). In this research, a microbiology laboratory of Alzahra Tehran University provided the resource of E. coli, and the resource of S.one was purchased from Academic Center for Education Culture and Research (ACECR). Since their life span is not enough for long-term use, they had to be cultured. For this reason, the bacteria were cultured on an agar plate and then, the plate was placed in an oven at 28 centigrade for 24 hours.

2.9. Test Procedure

For running the test in a batch feed mode, first, a colony of the bacterium was collected with a loop, and the bacterium was dissolved in a 9% sodium chloride solution (the amount of 9% sodium chloride solution varied depending on the bacterial concentration) under a fume hood to prepare the cell electrolyte. Then, a solution containing 100 ml of the substrate and 50 ml of the reducing agent was added to the electrolyte. Next, the chamber was placed on a hot plate, and a magnetic stirrer was in the chamber to prevent material deposition. Figure 6 shows an open-circuit setup.

A Hioki DT4200 series digital data logger was used that could be connected to a computer and it automatically recorded the voltage at predefined intervals. Therefore, a circuit was made via the cables of the data logger. It is worth mentioning that the measured voltages were used to calculate the current and power density via Equations (1) and (2) (Imologie et al., 2016).

$$I = \frac{V}{R} \tag{1}$$

$$P = \frac{V^2}{A_{an}R} \tag{2}$$

where V is the voltage across each resistor (mV), R is the resistance of each external load (Ω), I is the current (mA), P is the power density (mW/m^2), and A_{an} is the anode surface area (m^2).
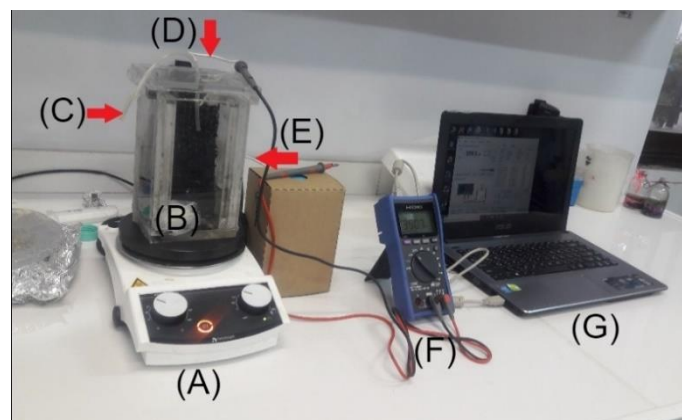

Figure 6. Setup of the batch feed mode test
(A) hot plate, (B) MFC, (C) N_2 gas tube, (D) wire of cathode, (E) wire of anode, (F) data logger, and (G) host computer

Two cables of data loggers were connected to a known resistor by two copper wires. Variable resistors (500, 1000 Ω, 2500 Ω, 7500 Ω, 15000 Ω) were used to find the highest power density and after 24 hours of recording data, another resistor was set up.

Table 2 shows a list of the devices and sensors from the beginning to the end of the experimentation.

Table 2. list of devices and sensors

Device/Sensor Name	Measured Variables	Error Range	Manufacturer Name
PH Meter	0-14	±0.001	Phoenix
Hot Plate	100-1400 rpm Up to 300 ℃	±0.02	Heidolph
Data Logger	1000 V	±0.001	Hioki
Scale	200 g	0.1 mg	Aczet

3. RESULTS AND DISCUSSION

This section represents the results of parameter studies that include the effects of bacteria type, chamber temperature, bacteria concentration, distance of electrodes, and stirrer speed on the cell polarization curve. In addition, for each parameter, the measurements are compared with the results reported by other researchers.

3.1. Bacteria Type

Bacterium is a catalytic agent in the electrochemical reactions in microbial fuel cells that attaches to the surface of an anode electrode and forms a biofilm (Flimban et al., 2019). Micro-organisms constituting the biofilm show considerable effects on the electron generation mechanism (Angelaalincy et al., 2018). Therefore, selecting a more efficient bacterium leads to more electron transfer to the external circuit (Bhargavi et al., 2018). S.one can provide its electron shuttles (Lee & Huang, 2013), and E. Coli has a greatly porous construction (Priya et al., 2016). Figure 7 shows the polarization curve for each bacterium.
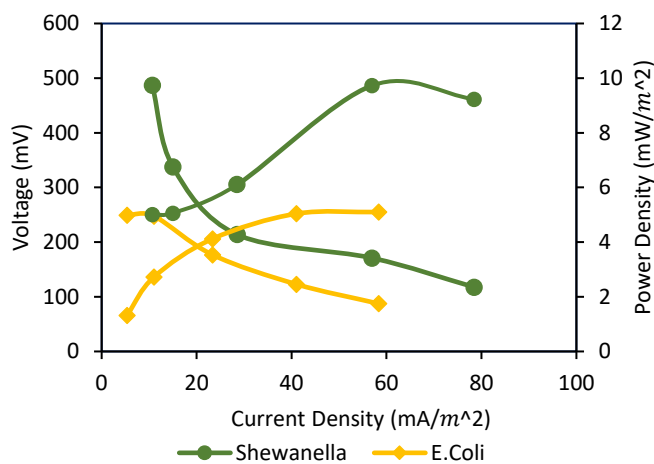

Figure 7. Comparison in the polarization curve of S. One and E. Coli bacteria

Based on Figure 7, due to more electron absorption in S. one bacteria than in E. coli, Shewanella generated more current at a given voltage. The maximum voltage at 7500 Ω external resistance was 486.9 mV for Shewanella and 249.4 mV for E. Coli. In addition, for Shewanella, the greatest power density was 9.73 mW/m² and at this point, the current density was 57 mA/m², while for E. Coli, the maximum power density was 5.1 mW/m² and at this point, the current density was 41 mA/m². The reason could be Shewanella feature of facultative anaerobic electrogenic (Sen-Dogan et al., 2020). The results are similar to those obtained by Juliastuti et al. (2017) upon comparing the capability to generate voltage for Shewanella and E. Coli in different bacteria concentrations for 12 days. In fact, for Shewanella, they found that the highest voltage was 988 mV at 12.5% (v/v), while the lowest voltage was around 450 mV at 10% (v/v). Besides, for E. Coli, the maximum voltage was 487 mV at 12.5% (v/v), while the minimum voltage was 150 mV at 17.5% (v/v). Moreover, Juliastuti et al. (2017) determined the greatest power density of Shewanella and E. Coli at 0.432 mW/m² and 0.371 mW/m², respectively . However, Cao et al. (2019) reported that the power density for E. Coli and Shewanella was 1304 mW/m² and 249 mW/m², respectively . The different shapes of the chamber may cause diverse outcomes. Wang et al. (2015) demonstrated that in a dual-chamber U-tube cell, the current density in S.one was higher than that in E. Coli.

3.2. Chamber Temperature

Temperature and the rate of reaction are the factors that highly impact microbial metabolic activity (Sen-Dogan et al., 2020; Singh & Krishnamurthy, 2019). Therefore, the second studied parameter was the chamber temperature. Therefore, the chamber was placed on a hot plate at three different temperatures, 30℃, 45℃, and 60℃, for 24 hours. Figure 8 shows the polarization curves at different temperatures.
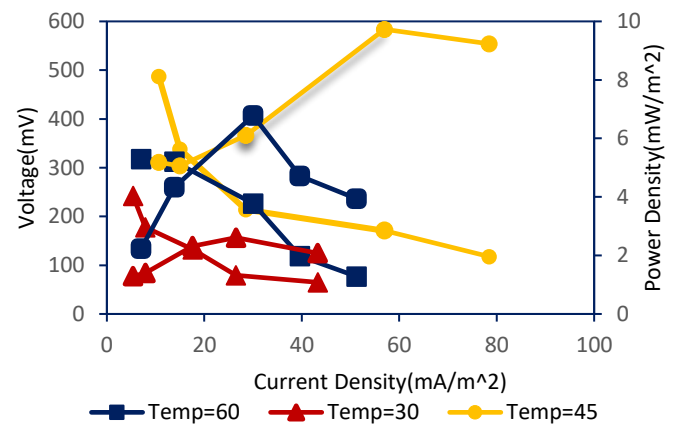

Figure 8. Comparison of the polarization curve of S. One at three different temperatures

Figure 8 shows that the highest voltage was 486.9 mV at 45℃; the next highest voltage was 317.8 mV at 60 ℃; and the lowest voltage was 242 mV at 30 ℃ with 7500 Ω external resistance. Furthermore, the maximum power density was 9.73 mW/m² at 45 ℃; the next highest power density was 6.78 mW/m² at 60 ℃; and the minimum power density was 2.61 mW/m² at 30 ℃. The maximum power density was a reference point for each temperature; the current density was 57 mA/m², 30 mA/m², and 26.5 mA/m² at 45 ℃, 60 ℃, and 30 ℃, respectively, in that order. Feng et al. (2019) divided six domestic wastewater reactors into three groups operating in the batch mode at 15℃, 20℃, and 30℃. They found that the maximum voltages at 30 ℃, 20 ℃, and 15 ℃ were 434.3 mV, 382.8 mV, and 297.0 mV, respectively. They also reported the highest power density at 30 ℃, 20 ℃, and 15 ℃ with 367.7 mW/m², 260.1 mW/m², and 166 mW/m², respectively. Aghababaie et al. (2015) investigated the generated power density at 30 ℃, 40 ℃, and 50 ℃. They found that the power density at 40 ℃ was twice that at 30 ℃ and the power density at 50 ℃ was reduced four times. Ren et al. (2017) built a miniaturized microbial fuel cell using Geobacter sulfurreducens and an anode of 150 µl. Next, Ren et al. placed the MFC in a temperature-controlled closed-loop oven to form the biofilm and waited for 3 to 6 hours to stabilize the current. First, they set the temperature at 41 ℃ and, then, measured the power of the MFC at different temperatures, 21℃ to 59 ℃, at six intervals. They found that the current

density at 21 °C was 2.2 A/m², while the parameter at 59 °C was 6.2 A/m². Gadkaria et al. (2020) observed the performance of five air-cathode MFCs at different temperatures. They used two methods namely parameter estimation at 24 °C, 30 °C, and 34 °C and numerical prediction at 20 °C and 40 °C to prove the applicability and accuracy of the experimental data. They then compared the results of their experimental data at 20 °C, 24 °C, 30 °C, 34 °C, and 40 °C with the results of the two methods. They obtained experimental and numerical predictions, which showed a 4.5% decrease in the maximum power density at 40 °C compared to 34 °C. Oliot et al. (2017) studied an MFC operation of an acetate batch. At 25 °C, it took 40 days to create three acetate batches, whereas only 20 days were sufficient at 40 °C. They found that the current density at 40 °C and 25 °C was 22.9 ± 4.2 A/m² and 9.4 ± 2 A/m², respectively. Table 3 shows a summary of the data.

Table 3. An overview of temperature comparison in different studies

Author Research Year	Temperature Range (°C)	Temperature of Max Voltage (°C) Max Voltage (mV)	Temperature of Max Power Density (°C) Max Power density (mW/m²)	Temperature of Max Current Density (°C) Max Current density (mA/m²)
Feng et al. 2019	15, 20,30	30 434.3 mV	30 367.7	
Aghababaie et al. 2015	30,40,50	- 650	40 2-fold than 30 °C	
Ren et al. 2017	21,49,53			49 6.2×10^3
Gadkari et al. 2020	20,25,30,34, 40	32.24 680	34 1.1x10^3	
Oliot et al. 2017	25,40			40 (22.9 ± 4.2) ×10^3
Current Work 2021	30,45,60	45 486.9	45 9.73	

3.3. Bacteria Concentration

Although the number of bacteria in a substrate is directly relevant to the power output in microbial fuel cells (Al-Asheh et al., 2020), the point is that a high concentration of bacteria does not have a positive impact on electricity generation

(Marashi & Kariminia, 2015). Hence, to find the most efficient concentration of bacteria, the cell performance was surveyed at three different concentrations: 0.5% (v/v) (4.5 mg/ml), 1% (v/v) (9mg/ml), and 1.5% (v/v) (13.5mg/ml). Figure 9 shows the polarization curves.
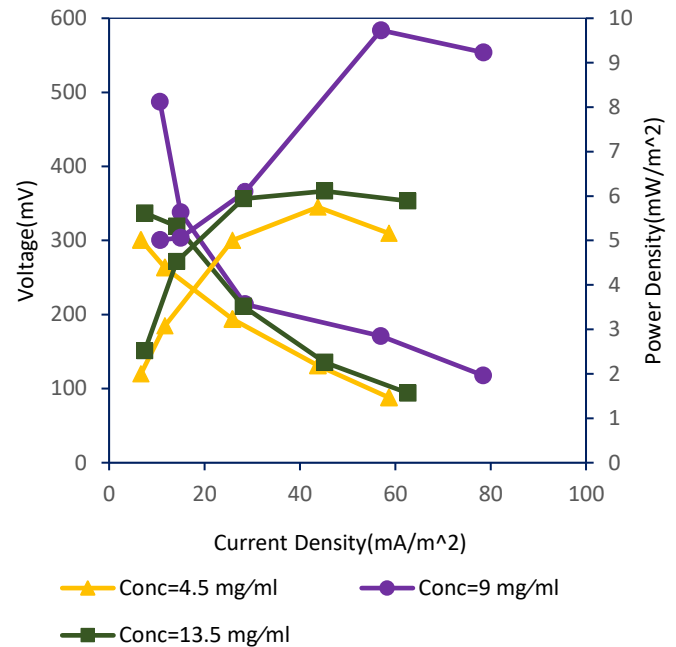

Figure 9. Comparison of the polarization curve of S. One at three different concentrations

Figure 9 illustrates that having more bacteria does not increase efficiency, and vice versa; thus, an optimal concentration should be sought. As can be seen, the maximum voltage at external resistance of 7500 Ω was 486.9 mV at 1%, the second 300 mV at 1.5%, and the lowest 337 mV at 0.5% concentration. Besides, the maximum power density was 9.73 mW/m² at 1% and at this point, the current density was 57 mA/m²; the next highest power density level was 6.11 mW/m² at 1.5%; the current density was 45.16 mA/m²; the lowest power density was 5.75 mW/m² at 0.5%; and the current density was 43.8 mA/m². Since at a concentration of 1.5%, the bacteria accumulate on the electrode surface and at a 0.5% concentration, there are not enough bacteria to absorb extra electrons, contributing to power generation; thus, the efficiency of the microbial fuel cell declines. Miyahara et al. used a single MFC with three equipped units and a cassette electrode. Meidensha et al. (2015) achieved MFC power density rates at different NaCl concentrations, mimicking freshwater (0 M), brackish water (0.05–0.3 M), seawater (0.6 M), and hypersaline lakes (1.8 M). They demonstrated that the highest and lowest power densities at 0.1M and 1.8M were 504 ± 41 mW/m² and 1.6 ± 0.3 mW/m², respectively.

Juliastuti et al. (2017) compared the capability of generating voltage for Shewanella and E. Coli at different bacteria concentrations of 10%, 12.5%, 15%, and 17.5% (v/v) for 12 days. In fact, they found that the highest voltage was 988 mV at 12.5% (v/v) while the lowest voltage was around 450 mV at 10% (v/v) for Shewanella; and the maximum voltage was 487 mV at 12.5% (v/v) and the minimum voltage was 150 mV at 17.5% (v/v) for E. Coli. Moreover, Juliastuti et al. (2017) found that the maximum power density for Shewanella and E. Coli was 0.432 mW/m² and 0.371 mW/m², respectively, at 12.5% (v/v). Tan et al. (2020) perused the function of a single-chamber UFML-MFC at different sodium acetate concentrations (0.405 g/L, 0.810 g/L, 1.215 g/L, 1.620 g/L). They grasped that the most efficient substrate concentrations were 0.810 g/L, while the maximum voltage was 610 mV, the greatest power density was 162.59 mW/m², and the current density was 468.74 mA/m². Ni et al. (2020) studied the operation of four identical double-chambered MFCs at 30 and three concentrations of swine wastewater. To stabilize the operation for two weeks, they found that the power density increased by growing concentration. Kong et al. (2018) studied the impact of glucose concentration on a two-chambered microbial fuel cell. His report indicated that the maximum volumetric power density decreased from 5.3 to 2.25 mW/m³ if the glucose concentration increased from 0.5 to 4 g/l and there was no power output when the glucose concentration reached 12 g/l.

3.4. Electrode Distance

Finding an efficient distance between the electrodes to obtain the best power density is quite significant (Harimawan et al., 2018). Therefore, the position of the anode with respect to that of the cathode was changed according to the following distance: 2 cm, 3 cm, and 4 cm, to study the impact of the distance variation. Figure 10 shows the polarization curves.
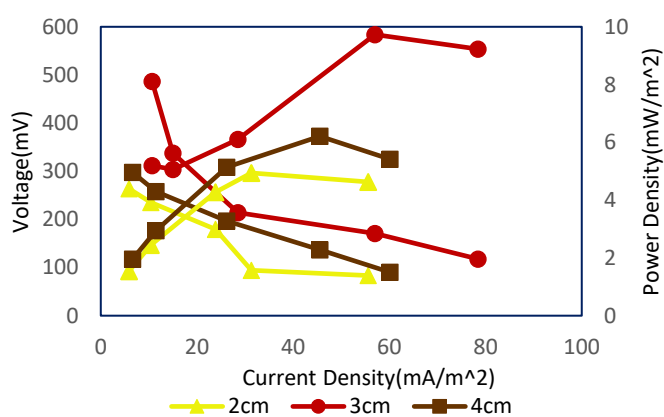

Figure 10. Comparison of the polarization curve of S. One at three different distances

As shown in Figure 10, the maximum voltage at 7500 Ω external resistance was 486.9 mV at 3 cm, the second highest voltage was 297.6 mV at 4 cm; and the lowest voltage was 263.7 mV at a 2 cm distance. Figure 10 indicates that the highest power density at a 3 cm distance was 9.73 mW/m², while the current density at this point was 56.97 mA/m². The

second power density was 6.21 mW/m² at a 4 cm distance, while the current density at this point was 45.53 mA/m²; the lowest power density was 4.94mW/m² corresponding to a 2 cm distance, while the current density at this point was 31.33 mA/m². At a very close distance, there is not sufficient space for electron transfer, and at a long distance, the ability to transmit electrons through the membrane is attenuated. Sing-Mei Tan et al. perused the influence of anode distributions (11cm, 17cm, 23cm) in a continuous up-flow MFC. They obtained that the highest voltage and power densities were 610.4 mV and 162.59 mW/m² at 23 cm; the next voltage and power density were 597 mV and 154.3 mW/m² at 17 cm; and the minimum voltage and power density were 584 mV and 140.85 mW/m² at 11 cm. González-Gamboa et al. (2018) studied a set of BMFCs with floating air cathodes at different distances and used the sediment of a bay as a substrate. They compared the distance between electrodes at 5 cm, 10 cm, 50 cm, and 100 cm. They obtained that the maximum power density was 109.6 mW/m² and the current density was 929.7 mA/m² in the BMFC at 10 cm anode depth and 10 cm of cathode separation. However, Gadkari et al. (2020) studied the operation of an MFC at 1 cm, 2 cm, 3 cm, and 4 cm distances between anode and cathode. They achieved that if the distance between the electrodes increased, the power density decreased. Lee and Huang (2013) examined electricity generation in a microbial fuel cell at 5.8 cm, 10.2 cm, 15.1 cm, and 19.5 cm electrode spacing. They discharged the MFC reactor continuously with a specific acetate concentration for at least seven days at room temperature for each run to maintain steady-state conditions. They demonstrated that the best power density was 3.32 mW/m² at 5.8 cm electrode spacing. Table 4 shows a summary of the data.

Table 4. An overview of comparison of electrodes distance in different studies

Author Research Year	Electrodes Distance (cm)	Distance of Max Voltage (cm) Max Voltage (mV)	Distance of Max Power Density (cm) Max Power density (mW/m²)
Tan et al. 2020	11,17,23	23 610.4mV	23 162.59
González-Gamboa et al. 2018	5,10,50,100		10 109.6
Gadkari et al. 2020	1,2,3,4		- increased as the distance decreased
Lee and Huang 2013	5.8,10.2,15.1,19.5		5.8 3.32
Current Work 2021	2,3,4	3 486.9	3 9.73

3.5. Stirrer Speed

The last parameter studied was the rotational speed of the magnetic stirrer placed in the substrate chamber. The rate of speed was set at three different values, i.e., 150, 200, and 250 rpm. Figure 11 shows the polarization curves.
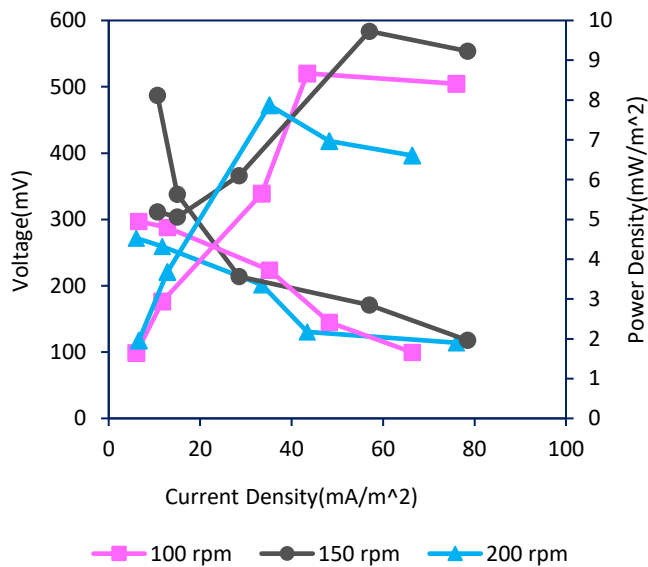

Figure 11. Comparison of the polarization curve of S. One at three different rotational speeds

As can be seen in Figure 11, the highest voltage at 7500 Ω external resistance was 486.9 mV at 150 rpm and the next was 297.1 mV at 100 rpm, while the lowest was 271.8 mV at 200 rpm. Moreover, the highest power density at 150 rpm was 9.73 mW/m^2, while the current density at this point was 56.97 mA/m^2. The second power density was 8.67 mW/m^2 corresponding to 100 rpm, while the current density was 43.43 mA/m^2. The lowest power density was 7.87 mW/m^2 corresponding to 200 rpm, while the current density at this point was 35.17 mA/m^2. What stands from the results is that a low rotational speed of the magnetic stirrer causes substrate stagnation; thus, the ability of bacteria to transfer electrons to the anode electrode is diminished. On the other hand, at a high rotational speed, no sufficient time is there for bacteria to move a considerable number of electrons to the anode electrode.

Pan et al. (2019) compared current density and power density at different anolyte circulation in a tubular MFC, 0 rpm, 150 rpm, and 300 rpm. They figured out that the maximum power density was 7.71±0.40 W/m^3 14.95±0.28 at 300 rpm, while the minimum power density was 5.03±0.43 W/m^3 at 0 rpm. However, there was no remarkable difference between the power density at 300 rpm and 150 rpm. Liu et al. (2020) considered different masses of carbon granules as an anode electrode in a double chamber microbial fuel cell to investigate the effect of the rotational rate of the carbon granules suspense. They studied different masses of carbon granules with 0 rpm,

50 rpm, 100 rpm, 150 rpm, 200 rpm, 250 rpm, and 300 rpm rotational rates. They concluded that as the rotational rate increased, the power density grew. Hamed et al. (2020) studied the effect of agitation and aeration of anolyte and catholyte at 0rpm, 150 rpm, 300 rpm, and 600 rpm on current density. They found that at 600 rpm, the current density in the catholyte increased by 2.2 times, while it decreased in the anolyte. Moreover, they reported that with aeration and agitation simultaneously, the current density significantly increased. However, the high agitation speed with aeration makes small air bubble dispersion in the catholyte, contributing to reduced electrical conductivity and current density.

4. CONCLUSION AND FUTURE RESEARCH

Microbial fuel cells could produce clean energy from various sustainable resources. However, it is critical to optimize their design and conditions to improve the performance of this technology. In this work, the impacts of parameters, such as bacterial type, chamber temperature, bacteria concentration, electrode space, and rotation speed of the substrate, were evaluated to determine the efficient power density for a single-chamber MFC device. The performance of the MFC was influenced by several factors according to the following results:

- S. one has a greater ability to absorb electrons than E. coli under the same conditions.

- Increasing the chamber temperature resulted in the bacteria going to the death log, and decreasing the chamber temperature led to the inability of the bacteria to transfer enormous electrons.

- In terms of bacterial concentration, an increase helps accumulate bacteria on the electrode surface, while a decrease leads to a fall in the number of electrons transferred.

- An increase in electrode space led to a decrease in the number of transferred electrons, while a decrease caused insufficient space for electron migration.

- Regarding the substrate rotation speed, the increase contributes to the formation of air bubbles, while the reduction contributes to the substrate sedimentation.

In Summary, providing S. one as a bacterium, 45 ℃ of chamber temperature, 1% bacteria concentration, 3 cm distance of electrodes, and 150 rpm substrate rotational speed contributed to the highest voltage and power density. The maximum voltage and the highest power density were 486.9 mV and 9.73 mW/m^2, respectively. In addition, at constant resistance, the system first went through incremental phase and then, reached the stationary phase over time. This study evaluated the effects

of different parameters on an MFC to optimize the performance, but future research must be conducted. Investigating other types of bacteria or even the mixture of E. coli and S.one may give better results. It is proposed to study (i) what happens after 24 hours of the experimentation, (ii) when the death phase of bacteria is at different temperatures, and (iii) how the pattern of biofilm structure forms at different concentrations. For future development, these assumptions will be taken into consideration.

5. ACKNOWLEDGMENT

Declaration of Competing Interest

The authors declare that they have no known competing financial interests or personal relationships that could have appeared to influence the work reported in this paper.

Funding

Competing interests

The authors declare that they have no competing interests.

NOMENCLATURE

MFC	Microbial Fuel Cell
PTFE	Polytetrafluoroethylene
A_{an}	Anode surface area (m²)
I	Current (mA)
P	Power density (mW/m²)
R	Resistance of each external load (Ω)
V	Voltage across each resistor (mV)

REFERENCES

1. Aghababaie, M., Farhadian, M., Jeihanipour, A., & Biria, D. (2015). Effective factors on the performance of microbial fuel cells in wastewater treatment. *Environmental Technology Reviews, 4*(1), 71-89. https://doi.org/10.1080/21622515.2015.1126235

2. Al-Asheh, S., Al-Assaf, Y., & Aidan, A. (2020). Single-chamber microbial fuel cells' behavior at different operational scenarios. *Energies, 13*, 5458. https://doi:10.3390/en13205458

3. Angelaalincy, M. J., Krishnaraj, R.N., G, S., Ashokkumar, B., Kathiresan, S. & Varalakshmi, P. (2018). Biofilm Engineering Approaches for Improving the Performance of Microbial Fuel Cells and Bio Electrochemical Systems. *Frontiers in Energy Research, 6.* https://doi.org/10.3389/fenrg.2018.00063

4. Bhargavi, G., Venu, V. & Renganathan, S. (2018) Microbial fuel cells: recent developments in design and materials. *IOP Conf. Series: Materials Science and Engineering, 330*, 012034. https://doi.org/10.1088/1757-899X/330/1/012034

5. Cao, Y., Mu, H., Liu, W., Zhang, R., Guo, J., Xian, M., & Liu, H. (2019). Electricians in the anode of microbial fuel cells: pure cultures versus mixed communities. *Microbial Cell Factories*, *18*, Article 39. https://doi.org/10.1186/s12934-019-1087-z

6. Chhazed, A. J., Makwana, M. V., & Chavda, N. K. (2019). Microbial Fuel Cell Functioning, Developments and Applications. *International Journal of Scientific & Technology Research*, *8*(12). http://www.ijstr.org/final-print/dec2019/Microbial-Fuel-Cell-Functioning-Developments-And-Applications-a-Review-.pdf

7. Cui, C. Y. (2016). The effect of anode surface structures on microbial fuel cells (Master's thesis). Retrieved from https://kb.osu.edu/bitstream/handle/1811/76443/CuiClare_Thesis_Final.pdf?sequence=1

8. Dessie, Y., Tadesse, S., & Eswaramoorthy, R. (2020). Review on manganese oxide-based biocatalyst in microbial fuel cell: Nanocomposite approach. *Materials Science for Energy Technologies*, *3*(4), 136-149. https://doi.org/10.1016/j.mset.2019.11.001

9. Ezziat, L., Elabed, A., Ibnsouda, S. K., & El Abed, S. (2019). Challenges of Microbial Fuel Cell Architecture on Heavy Metal Recovery and Removal from Wastewater. *Frontiers in Energy Research, 7*, 1. https://doi.org/10.3389/fenrg.2019.00001

10. Feng, Y., Lee, H., Wang, X., & Liu, Y. (2019). Electricity generation in microbial fuel cells at different temperature and isolation of electrogenic bacteria. In *Asia-Pacific Power and Energy Engineering Conference*. https://www.researchgate.net/publication/224444633

11. Flimban, S. G. A., Kim, T., Ismail, I. M. I., & Oh, S. (2019). Overview of Recent Advancements in the Microbial Fuel Cell from Fundamentals to Applications: Design, Major Elements, and Scalability. *Energies 2019, 12*(17), 3390. https://doi.org/10.3390/en12173390

12. Gadkari, S., Fontmorin, J.-M., Yu, E., & Sadhukhan, J. (2020). Influence of temperature and other system parameters on microbial fuel cell performance: Numerical and experimental investigation. *Chemical Engineering Journal, 388*, 124176. https://doi.org/10.1016/j.cej.2020.124176

13. Gajda, I., Greenman, J., & Ieropoulos, I. (2020). Microbial Fuel Cell stack performance enhancement through carbon veil anode modification with activated carbon powder. *Applied Energy*, *262*, 114475. https://doi.org/10.1016/j.apenergy.2019.114475

14. González-Gamboa, N., Domínguez-Benetton, X., Pacheco-Catalán, D., Kumar-Kamaraj, S., Valdés-Lozano, D., Domínguez-Maldonado, J., & Alzate-Gaviria, L. (2018). Effect of operating parameters on the performance evaluation of benthic microbial fuel cells using sediments from the Bay of Campeche. *Journal of Sustainability, 10*. https://doi:10.3390/su10072446

15. Greenman, J., Mendis, B. A., Gajda, I., & Ieropoulos, I. A. (2022). Microbial fuel cell compared to a chemostat. *Chemosphere, 296*, 133967. https://doi.org/10.1016/j.chemosphere.2022.133967

16. Hamed, M. S., Majdi, H. S., & Hasan, B. O. (2020). Effect of electrode material and hydrodynamics on the produced current in double chamber microbial fuel cells. *ACS Omega, 5*, 10018-10025. https://DOI: 10.1021/acsomega.9b04451

17. Harimawan, A., Devianto, H., Al-Aziz, R. H. R. M. T., Shofinita, D., & Setiadi, T. (2018). Influence of electrode distance on electrical energy production of microbial fuel cell using tapioca wastewater. *Journal of Engineering and Technological Sciences, 50*(6), 841-855. https://doi: 10.5614/j.eng.technol.sci.2018.50.6.7

18. Imologie, S. M., Raji, O. A., Agidi, G., & Shekwaga, C. A. O. (2016). Performance of a Single Chamber Soil Microbial Fuel Cell at Varied External Resistances for Electric Power Generation. *Journal of Renewable Energy and Environment, 3*, 53-58. https://doi.org/10.30501/jree.2016.70092

19. Juliastuti, S. R., Darmawan, R., Ayuningtyas, A., & Ellyza, N. (2017). The utilization of Escherichia coli and Shewanella oneidensis for microbial fuel cell. In *The 3rd International Conference on Chemical Engineering Sciences and Applications IOP*, *34*, 20-21. http://dx.doi.org/10.1088/1757-899X/334/1/012067

20. Jumma, S. & Patil, N. (2016). Microbial Fuel Cell: Design and Operation. *Journal of Microbiology and Biotechnology*, Special Issue, Reviews on Microbiology. https://www.researchgate.net/publication/308333548

21. Keshavarz, M., Mohebbi-Kalhori, D., & Yousefi, V. (2022). Multi-response optimization of tubular microbial fuel cells using response surface methodology (RSM). *Journal of Renewable Energy and Environment (JREE)*, *9*(2), 49-58. https://doi.org/10.30501/jree.2022.290677.1218

22. Kiaeenajad, A., Moqtaderi, H., Mahmoodi, N., Maerufi, S. (2020). Design and Construction of a Microbial Fuel Cell for Electricity Generation from Municipal Wastewater Using Industrial Vinasse as Substrate. *Modares Mechanical Engineering, 20*(9), 2403-2412. http://mme.modares.ac.ir/article-15-38562-en.html

23. Kong, X., Yang, G., & Sun, Y. (2018). Performance investigation of batch mode microbial fuel cells fed with high concentration of glucose. *Journal of Scientific and Technical Research, 7*. https://DOI: 10.26717/BJSTR.2018.03.000864

24. Koók, L., Nemestóthy, N., Bélafi-Bakó, K., & Bakonyi, P. (2021). Treatment of dark fermentative H2 production effluents by microbial fuel cells: A tutorial review on promising operational strategies and practices. *International Journal of Hydrogen Energy, 46*(17), 5556–5569. https://doi.org/10.1016/j.ijhydene.2020.11.084

25. Lee, C.Y. & Huang, Y.N. (2013) The effects of electrode spacing on the performance of microbial fuel cells under different substrate concentrations. *Water Science and Technology, 68*(8), 1898-1902. https://doi.org/10.2166/wst.2013.446 PMID: 24225104

26. Li, S., Ho, S.H., Hua, T., Zhou, Q., Li, F. & Tang, J. (2021). Sustainable biochar as an electrocatalysts for the oxygen reduction reaction in microbial fuel cells. *Green Energy & Environment, 6*(4), 644-659. https://doi.org/10.1016/j.gee.2020.11.010

27. Liu, Y., Sun, X., Yin, D., Cai, L., & Zhang, L. (2020). Suspended anode-type microbial fuel cells for enhanced electricity generation. *RSC Advances, 10*, 9868-9877. https://DOI: 10.1039/c9ra08288c

28. Marashi, S. K. F., & Kariminia, H. R. (2015). Performance of a single chamber microbial fuel cell at different organic loads and pH values using purified terephthalic acid wastewater. *Journal of Environmental Health Science and Engineering, 13*. https://doi.org/10.1186/s40201-015-0179-x

29. Mateo, S., Cañizares, P., Rodrigo, M. A., & Fernandez-Morales, F. J. (2018). driving force behind electrochemical performance of microbial fuel cells fed with different substrates. *Chemosphere*, *207*. https://doi.org/10.1016/j.chemosphere.2018.05.100

30. Mei, X., Xing, D., Yang, Y., Liu, Q., Zhou, H., Guo, C., Ren, N. (2017). Adaptation of microbial community of the anode biofilm in microbial fuel cells to temperature. *Bioelectrochemistry, 118*, 8-15. https://doi.org/10.1016/j.bioelechem.2017.04.005

31. Meidensha, A.M.M., Kouzuma, A., & Watanabe, K. (2015). Effects of NaCl concentration on anode microbes in microbial fuel cells. *AMB Express, 5*. https://doi.org/10.1186/s13568-015-0123-6

32. Mishra, B., Awasthi, S. K., & Rajak, R. K. (2017). A review on electrical behavior of different substrates, electrodes and membranes in microbial fuel cell. *International Journal of Energy and Power Engineering*, *11*(9). https://doi.org/10.5281/zenodo.1132290

33. Nguyen, D.-T., Tamura, T., Tobe, R., Mihara, H., & Taguchi, K. (2020). Microbial fuel cell performance improvement based on FliC-deficient E. coli strain. *Energy Reports, 6*, 763–767. https://doi.org/10.1016/j.egyr.2020.11.133

34. Ni, H., Wang, K., Lv, S., Wang, X., Zhuo, L., & Zhang, J. (2020). Effects of concentration variations on the performance and microbial community in microbial fuel cell using swine wastewater. *Energies, 13*. https://doi.org/10.3390/su10072446

35. Obata, O., Salar-Garcia, M. J., Greenman, J., Kurt, H., Chandran, K., & Ieropoulos, I. (2020). Development of efficient electroactive biofilm in urine-fed microbial fuel cell cascades for bioelectricity generation. *Journal of Environmental Management, 258*, 109992. https://doi.org/10.1016/j.jenvman.2019.109992

36. Obileke, K. C., Onyeaka, H., Meyer, E. L., & Nwokolo, N. N. (2021). Microbial fuel cells, a renewable energy technology for bio-electricity generation. *Electrochemistry Communications*, *125*, 107003. https://doi.org/10.1016/j.elecom.2021.107003

37. Oliot, M., Erable, B., De Solan, M.-L., & Bergel, A. (2017). Increasing the temperature is a relevant strategy to form microbial anodes intended to work at room temperature. *Electrochemical Acta*, *258*, 134-142. https://doi.org/10.1016/j.electacta.2017.10.110

38. Páez, A., Lache-Muñoz, A., Medina, S., Zapata4, J., & Sánchez, O. (2019). Electric power production in a microbial fuel cell using Escherichia coli and Pseudomonas aeruginosa, synthetic wastewater as substrate, carbon cloth and graphite as electrodes, and methylene blue as mediator. *Laboratorio Escala*, 10(6). https://doi.org/10.24850/j-tyca-2019-06-11

39. Pan, Y., Zhua, T., & Heb, Z. (2019). Energy advantage of anode electrode rotation over anolyte recirculation for operating a tubular microbial fuel cell. *Electrochemistry Communications, 106,* 106529. https://doi.org/10.1016/j.elecom.2019.106529

40. Pandey, G. (2019). Biomass based bio-electro fuel cells based on carbon electrodes: an alternative source of renewable energy. *SN Applied Sciences*, *1*, 1-8. https://doi.org/10.1007/s42452-019-0409-4

41. Priya, R. L., Ramachandran, T., & Suneesh, P. V. (2016). Fabrication and characterization of high-power dual chamber E. coli microbial fuel cell. *Materials Science and Engineering, 149*, 012215. https://doi:10.1088/1757-899X/149/1/012215

42. Ren, H., Jiang, C., & Chae, J. (2017). Effect of temperature on a miniaturized microbial fuel cell (MFC). *Micro and Nano Systems, 5*, 13. https://doi.org/10.1186/s40486-017-0048-8

43. Salar-García, M. J., & Ieropoulos, I. (2020). Optimization of the internal structure of ceramic membranes for electricity production in urine-fed microbial fuel cells. *Journal of Power Sources*, *451*, 227741. https://doi.org/10.1016/j.jpowsour.2020.227741

44. Salar-García, M. J., Walter, X. A., Gurauskis, J., de Ramón Fernández, A., & Ieropoulos, I. (2021). Effect of iron oxide content and microstructural porosity on the performance of ceramic membranes as microbial fuel cell separators. *Electrochemica Acta*, 367, 137385. https://doi.org/10.1016/j.electacta.2020.137385

45. Şen-Doğan, B., Okan, M., Afşar-Erkal, N., Özgür, E., Zorlu, Ö., & Külah, H. (2020). Enhancement of the start-up time for microliter-scale microbial fuel cells (μMFCs) via the surface modification of gold electrodes. *Micromachines (Basel), 11*(7), 703. https://doi.org/10.3390/mi11070703

46. Simeon, I. M., Herkendell, K., Pant, D., & Freitag, R. (2022). Electrochemical evaluation of different polymer binders for the production of carbon-modified stainless-steel electrodes for sustainable power generation using a soil microbial fuel cell. *Chemical Engineering Journal Advances, 10*, 100246. https://doi.org/10.1016/j.ceja.2022.100246

47. Singh, A., & Krishnamurthy, B. (2019). Parametric modeling of microbial fuel cells. *Journal of Electrochemical Science and Engineering, 9*(4), 311-323. http://dx.doi.org/10.5599/jese671

48. Tabrizi, A., Aghajani, H., & Laleh, F. F. (2019). Review on the Materials for Hydrogen Adsorption & Storage. *Journal of Renewable Energy and Environment (JREE)*, *7*(2), 2-13. https://doi.org/20.1001.1.24234931.1399.7.2.2

49. Tan, S.M., Ong, S.A., Ho, L.N., Wong, Y.S., Thung, W.E., Teoh, T.P. (2020). The reaction of wastewater treatment and power generation of single chamber microbial fuel cell against substrate concentration and anode distributions. *Journal Environment Health Sci Eng, 18*(1), 793-807. https://doi.org/10.1007/s40201-020-00504-w. PMID: 33312603; PMCID: PMC7721755

50. Walter, X. A., You, J., Winfield, J., Bajarunas, U., Greenman, J., & Ieropoulos, I. A. (2020). From the lab to the field: Self-stratifying microbial fuel cells stacks directly powering lights. *Applied Energy*, *277*, 115514. https://doi.org/10.1016/j.apenergy.2020.115514

51. Wang, V., Sivakumar, K., Yang, L., & Nealson, K. H. (2015). Metabolite-enabled mutualistic interaction between Shewanella oneidensis and Escherichia coli in a co-culture using an electrode as electron acceptor. *Scientific Reports, 5*, 11222. https://doi:10.1038/srep11222